The role of homologous recombination in mitotic and meiotic double-strand break repair

Vries, Femke Adriana Theodora de

Appendix

Selected coloured figures

Chapter 3 Figure 2

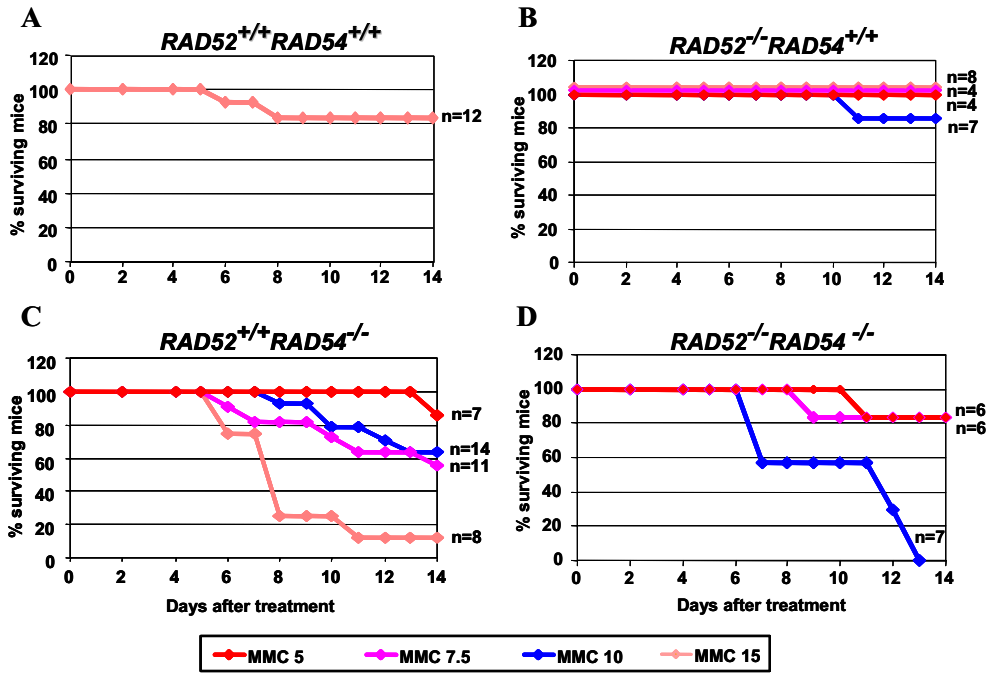

Figure 2: Survival of mice following mitomycine C treatment. Animals were injected intraperitoneally with 5, 7.5, 10 or 15 mg/kg bodyweight MMC. Total numbers of individually treated mice are indicated per dose. Control **(A)** *RAD52*$^{-/-}$ **(B)**, *RAD54*$^{-/-}$**(C)** and *RAD52*$^{-/-}$ / *RAD54*$^{-/-}$ **(D)** mice.

Chapter 3 Figure 4

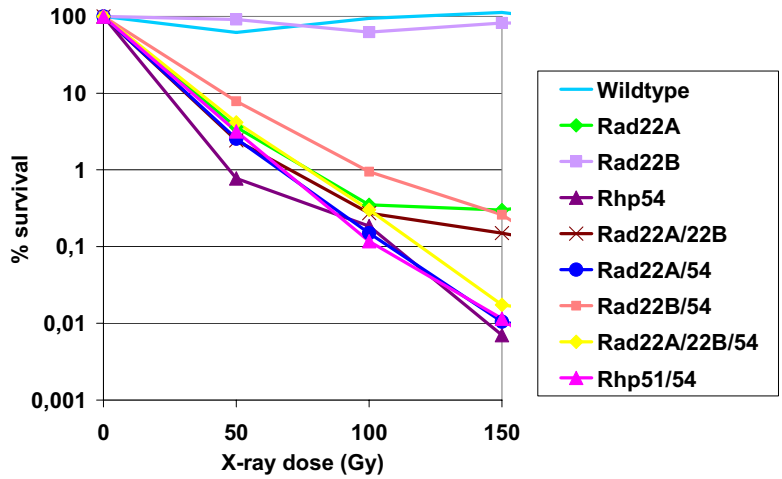

Figure 4: X-ray survival of wildtype and single, double and triple mutant S. *pombe* strains. Exponentially growing cells were harvested, irradiated and appropriate dilutions were plated in triplicate on YES media. After 3 days of incubation at 30°C the colonies were counted. Each survival experiment was repeated at least twice.

Chapter 4 Figure 4

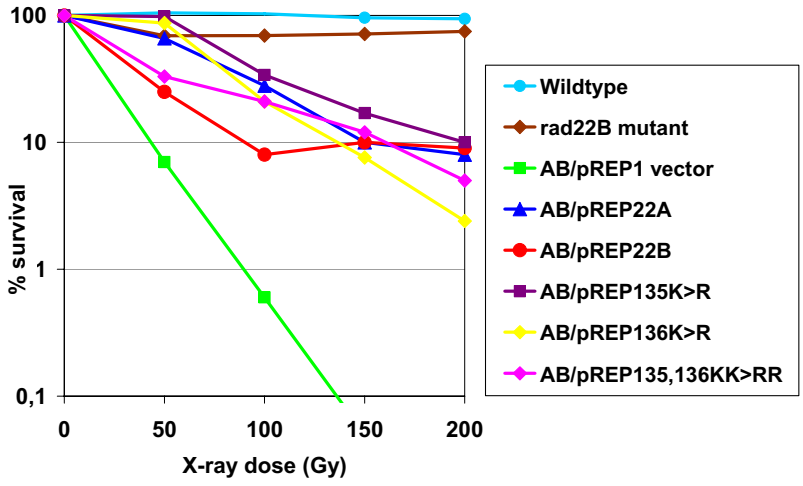

Figure 4: Survival of *S. pombe* strains after irradiation with X-rays. After irradiation of exponentially growing cells, appropriate dilutions were plated and colonies were counted after incubation of the plates for 3 days at 30ºC. Each survival experiment was repeated at least twice. Strains used in this experiment: wildtype (Y4), rad22B$^{-/-}$ (rad22B mutant), and double mutant rad22A$^{-/-}$rad22B$^{-/-}$ strains containing expression vectors without insert (AB/pREP-), with Rad22A insert (AB/pREP22A), with Rad22B insert (AB/pREP22B) and with Rad22A inserts in which the putative SUMO acceptor site has been mutated (AB/pREP135 K>R, AB/pREP136 K>R, AB/pREP135,136 KK>RR). For details see Materials and methods.

Chapter 5 Figure 2

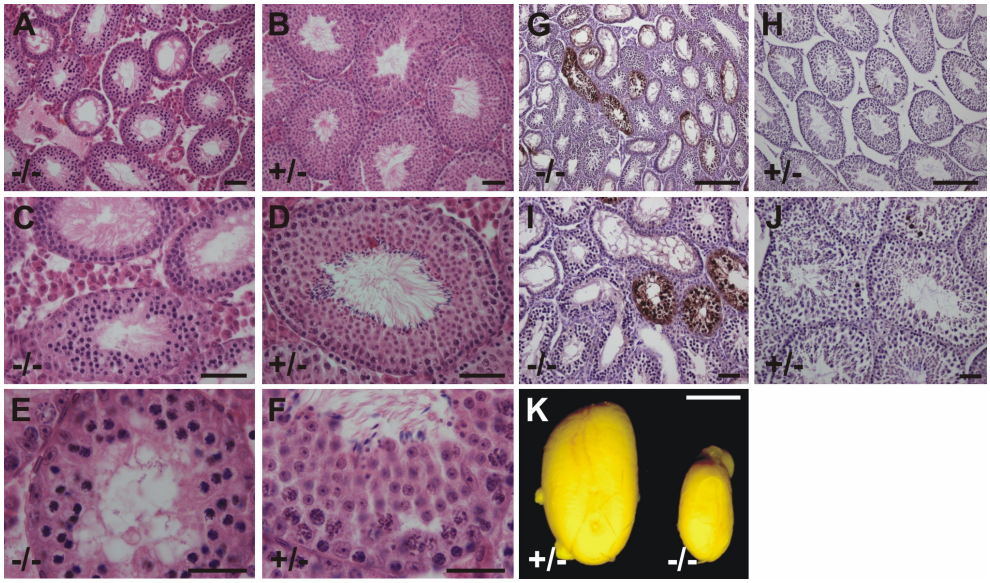

Figure 2: Morphology, histology and TUNEL analysis of testes from *Sycp1*$^{-/-}$ mice.
The histological sections were stained with haematoxilin and eosin. **(A-F)** Testicular histology of adult *Sycp1*$^{-/-}$ (-/-, **A,C,E**) and *Sycp1*$^{+/-}$ (+/-, **B,D,F**) mice. Note the total absence of postmeiotic germ cells in *Sycp1*$^{-/-}$ sections. Pachytene nuclei are abundant, but show aberrant nuclear morphology. **(G-J)** TUNEL analysis of testis sections of *Sycp1*$^{-/-}$ (-/-, **G,I**) and *Sycp1*$^{+/-}$ (+/-, **H,J**) mice. Tubule sections with numerous TUNEL-positive nuclei occur only in *Sycp1*$^{-/-}$ mice. A few apoptotic nuclei are visible in tubule sections from *Sycp1*$^{+/-}$ mice. **(K)** Testes from *Sycp1*$^{+/-}$ (+/-) and *Sycp1*$^{-/-}$ (-/-) mice. Bars: (**A-D,I,J**) 50 µm; (**E-F**) 25 µm; (**G-H**) 100 µm; (**K**) 2 mm.

Figure 3: Assembly of AEs in *Sycp1*$^{-/-}$ mice.
(A-B) Electron micrograhs of AEs and SCs from wildtype (+/+) and *Sycp1*$^{-/-}$ (−/−) male mice; (**A**) wildtype SC with closely apposed axial elements (AE) and a central element (CE); (**B**) homologously aligned axial elements (AE) from a *Sycp1*$^{-/-}$ spermatocyte, connected by axial associations (AA). **(C-J)** Components of AEs and SCs in wildtype (+/+) and *Sycp1*$^{-/-}$ (−/−) diplotene (**C**-**D**) or pachytene (**E**-**J**) spermatocytes; LE/AE protein SYCP3 and all analyzed cohesins are present in LEs/AEs of wildtype and mutant, whereas SYCP1 is not detectable in mutant spermatocytes. **(K-T)** formation of AEs/LEs, as shown by REC8/SYCP3 double labelling, in wildtype (+/+) and *Sycp1*$^{-/-}$ (−/−) spermatocytes; (**K**,**L**) early leptonema; (**M**,**N**) late leptonema; (**O**,**P**) zygonema; (**Q**,**R**) pachynema; (**S**,**T**) diplonema; note the XY bivalent (XY) in wildtype cells (**Q**,**S**), and separate X and Y chromosomes in the *Sycp1*$^{-/-}$ cells (**R**,**T**). Bars in (**A**-**B**) 1 µm; bars in (**C**-**T**) 10 µm.

Chapter 5 Figure 3

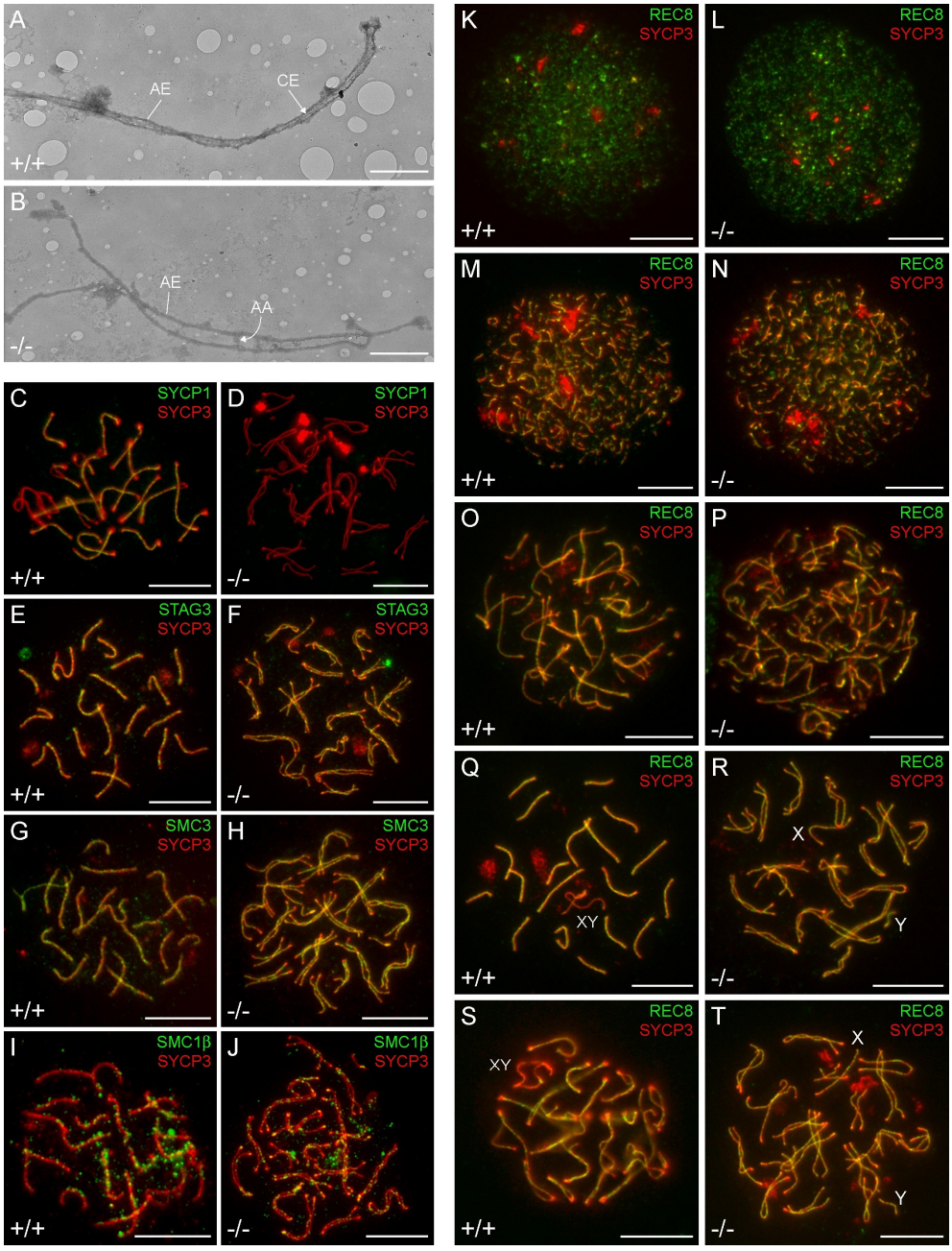

Legends figure 3: see page 175

Chapter 5 Figure 4

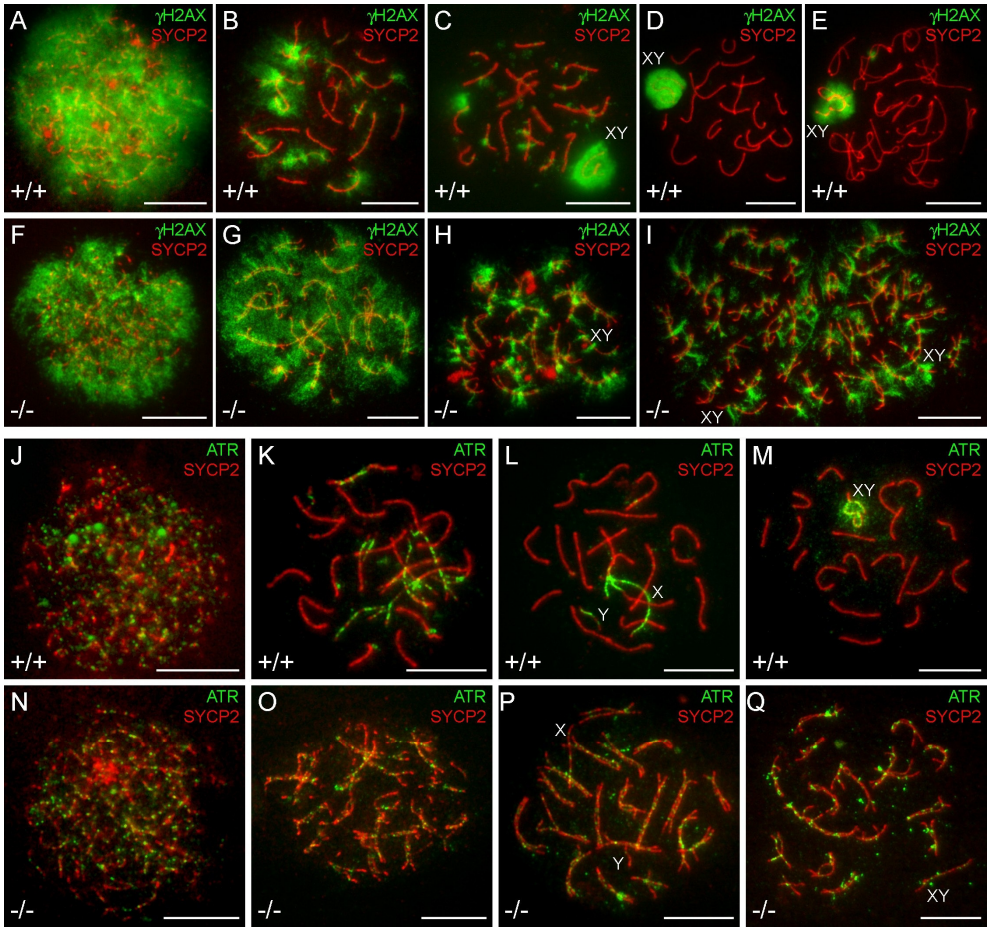

Figure 4: γH2AX and ATR in wildtype (+/+) and *Sycp1*$^{-/-}$ (−/−) spermatocytes.
(A-I) γH2AX ; (**A**,**F**) leptonema; (**B**,**G**) zygonema; (**C**) early pachynema; (**D**,**H**) mid-pachynema; (**E**,**I**) diplonema; the sex chromosomes (XY) form an XY-body in wildtype spermatocytes (**C**-**E**), but not in *Sycp1*$^{-/-}$ spermatocytes, even though the X and Y chromosomes are associated in the cells in (**H**) and (**I**). **(J-Q)** ATR; (**J**,**N**) leptonema; (**K**,**O**) zygonema; (**L**) early pachynema and (**M**) and (**P**) mid-pachynema; (**Q**) diplonema; ATR is present throughout the chromatin of the XY bivalent in wildtype spermatocytes (**M**), but forms foci and distinct domains along the X and Y chromosomes in *Sycp1*$^{-/-}$ cells (**P**-**Q**). Insets in (**J**) and (**N**) show the close association of ATR with the ends of AE fragments in wildtype (+/+) and *Sycp1*$^{-/-}$ leptonema. Bars 10 μm.

Chapter 5 Figure 5

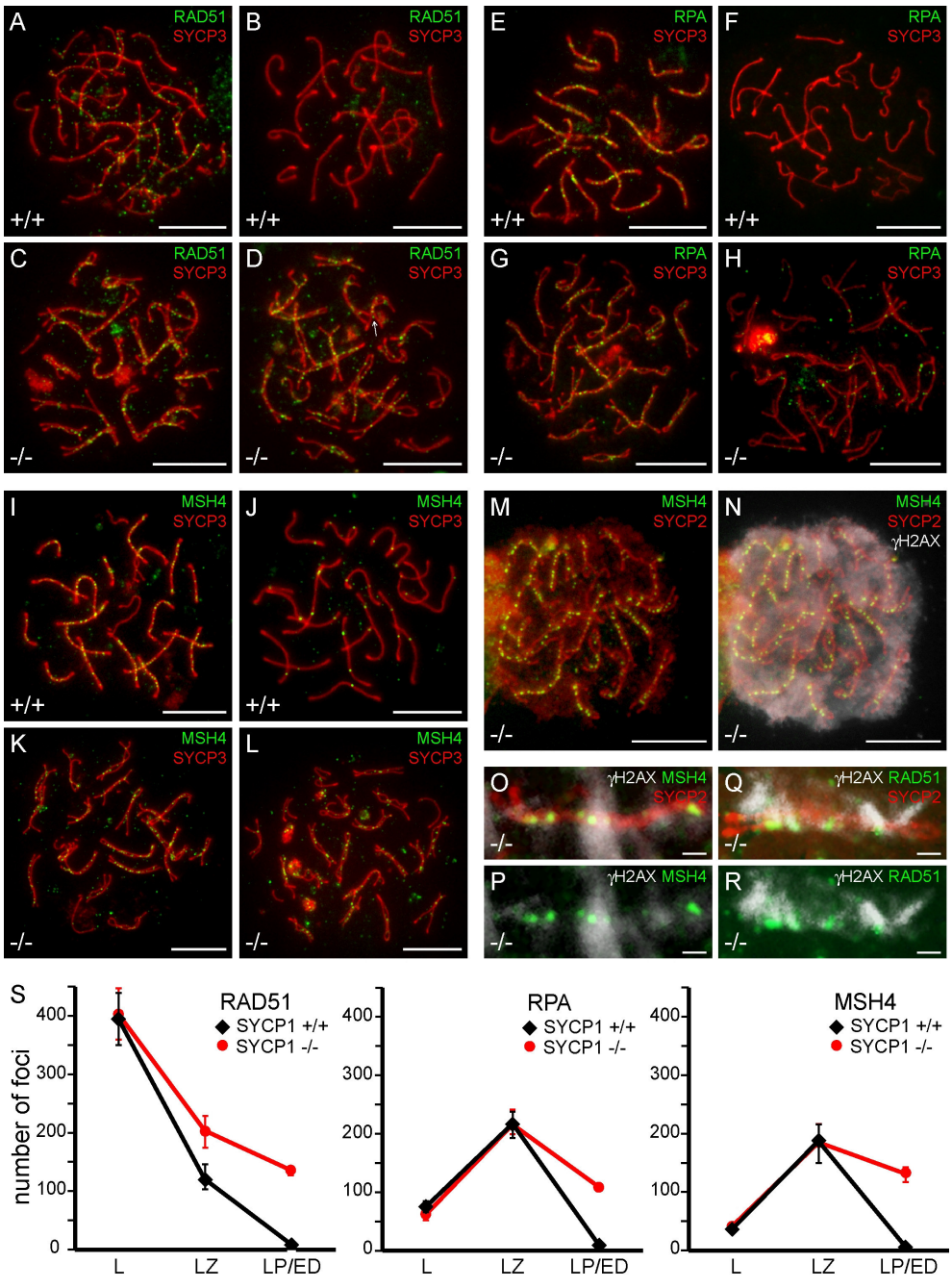

Legends figure 5: see page 179

Figure 5: Recombination-related proteins along AEs and SCs in wildtype (+/+) and *Sycp1*$^{-/-}$ (−/−) spermatocytes.
(A-D) RAD51/DMC1; (**A**,**C**) late zygonema; (**B**,**D**) late pachynema. **(E-H)** RPA; (**E**,**G**) late zygonema; (**F**,**H**) diplonema. **(I-L)** MSH4; (**I**,**K**) late zygonema; (**J**) mid-pachynema; (**L**), diplonema. **(M-N)** MSH4/SYCP2/γH2AX triple labelling of a zygotene *Sycp1*$^{-/-}$ spermatocyte; the number and localization of MSH4 foci appears normal, but the persistence of γH2AX throughout the chromatin is abnormal. **(O-P)** MSH4/ SYCP3/γH2AX triple labelling of a late pachytene *Sycp1*$^{-/-}$ bivalent, to show that part of the γH2AX domains co-localize with an MSH4 focus. **(Q-R)** RAD51/SYCP2/γH2AX triple labelling of a late pachytene *Sycp1*$^{-/-}$ bivalent, to show that part of the γH2AX domains co-localize with a RAD51 focus. **(S)** Counts of RAD51, RPA and MSH4 foci in successive stages of meiotic prophase; the vertical axes represent the number of AE or SC associated foci per cell; the vertical bars represent the observed range of the number of foci per cell in a given spermatocyte stage. For more details of the counts, see Supplementary Information, Fig. S4. Bars in (**A**-**N**) 10 μm; bars in (**O**-**R**) 1 μm.

Chapter 5 Figure 6

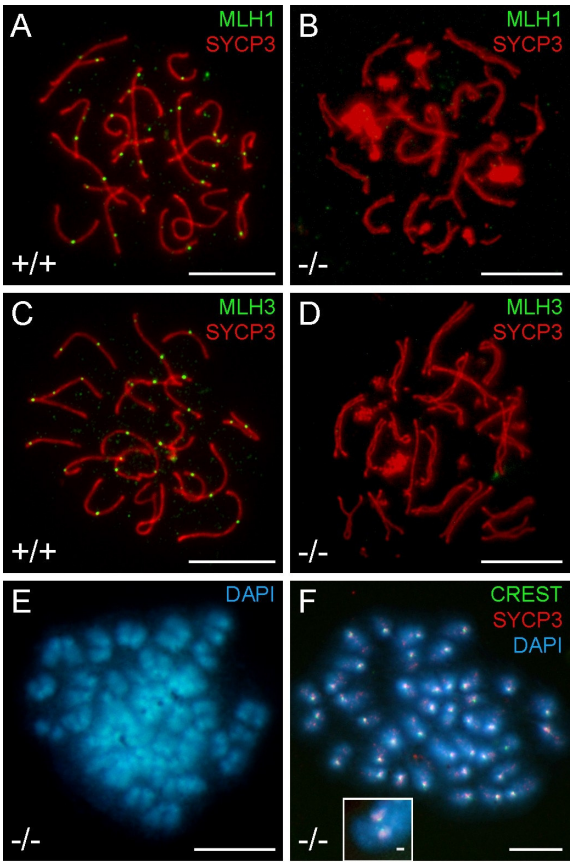

Figure 6: Formation of crossovers and chiasmata.
(A,B) MLH1 labelling and **(C,D)** MLH3 labelling of wildtype (+/+) or *Sycp1*$^{-/-}$ (−/−) pachytene spermatocytes. The *Sycp1*$^{-/-}$ spermatocytes do not assemble MLH1 or MLH3 foci. **(E,F)** A natural (**E**) and an okadaic acid-induced (**F**) metaphase I spermatocyte of *Sycp1*$^{-/-}$. In the cells shown here, only univalents can be identified; the inset in (**F**) shows a bivalent found in another OA-induced *Sycp1*$^{-/-}$ metaphase I. Bars in (**A**-**F**) 10 μm; bar in the inset in (**F**) 1 μm.